



## Original article

# Myeloperoxidase-mediated oxidation of edaravone produces an apparent non-toxic free radical metabolite and modulates hydrogen peroxide-mediated cytotoxicity in HL-60 cells

Lindsey Y.K. Suh<sup>a</sup>, Dinesh Babu<sup>a</sup>, Lusine Tonoyan<sup>a</sup>, Béla Reiz<sup>b</sup>, Randy Whittal<sup>b</sup>,  
S. Amirhossein Tabatabaei-Dakhili<sup>a</sup>, Andrew G. Morgan<sup>a</sup>, Carlos A. Velázquez-Martínez<sup>a</sup>,  
Arno G. Siraki<sup>a,\*</sup>

<sup>a</sup> Faculty of Pharmacy & Pharmaceutical Sciences, Katz Group-Rexall Centre for Pharmacy and Health Research, University of Alberta, Edmonton, Alberta, T6G 2E1, Canada

<sup>b</sup> Department of Chemistry, 11227 Saskatchewan Drive, University of Alberta, Edmonton, Alberta, T6G 2G2, Canada

## ARTICLE INFO

## Keywords:

Edaravone  
Myeloperoxidase  
Free radicals  
Electron spin resonance  
HL-60 cells  
Antioxidant

## ABSTRACT

Edaravone is considered to be a potent antioxidant drug known to scavenge free radical species and prevent free radical-induced lipid peroxidation. In this study, we investigated the effect of edaravone on the myeloperoxidase (MPO) activity, an enzyme responsible for the production of an array of neutrophil-derived oxidants that can cause cellular damage. The addition of edaravone to the reaction of MPO and hydrogen peroxide (H<sub>2</sub>O<sub>2</sub>) significantly enhanced the reduction of MPO Compound II back to native MPO. Interestingly, the MPO-mediated production of toxic hypochlorous acid exhibited a concentration-dependent biphasic effect, with the apparent optimal edaravone concentration at 10 μM. Oxidation of edaravone by MPO was examined by various analytical methods. An MPO-catalyzed product(s) of edaravone was identified at 350 nm by kinetic analysis of UV–Vis spectroscopy. Several MPO-catalyzed metabolites of edaravone were proposed from the LC-MS analyses, including oxidized dimers from edaravone radicals. Electron spin resonance (ESR) spin trapping detected a carbon-centred radical metabolite of edaravone. NMR studies revealed that there are two exchangeable hydrogens, one of which is on the α-carbon, justifying the carbon-centred edaravone radical produced from MPO. Despite the formation of an edaravone carbon-radical metabolite, it did not appear to effectively oxidize GSH (in comparison with phenoxyl radicals). Viability (ATP) and cytotoxicity (LDH release) assays showed a concentration-dependent effect of edaravone on HL-60 cells treated with either a bolus concentration of 30 μM H<sub>2</sub>O<sub>2</sub> or a flux of H<sub>2</sub>O<sub>2</sub> generated by 5 mM glucose and 10 mU/mL glucose oxidase. The H<sub>2</sub>O<sub>2</sub>-induced toxicity was ameliorated at high edaravone concentrations (100–200 μM). In contrast, low concentrations of edaravone (1–10 μM) exacerbated the H<sub>2</sub>O<sub>2</sub>-induced toxicity. However, the effect of edaravone at low concentration (0–10 μM) appeared more prominent with the LDH assay only. The cellular findings correlated with the biochemical studies with respect to hypochlorous acid formation. These findings provide interesting perspectives regarding the duality of edaravone as an antioxidant drug.

## 1. Introduction

Edaravone (3-methyl-1-phenyl-2-pyrazolin-5-one), marketed under the trade name Radicava® or Radicut®, is a small molecular weight drug with antioxidant properties. In 2001, edaravone was approved in Japan for the early treatment of acute cerebral infarction. Later, it was approved to slow the progression of amyotrophic lateral sclerosis (ALS) in Japan and the United States in 2015 and 2017, respectively [1]. It was just recently approved by Health Canada, in October 2018 [2].

It is believed that oxidative stress is involved in the pathobiology, which occurs after an ischemic stroke [3]. Oxidative stress is likely manifested by multiple processes, which produces reactive oxygen species (ROS) including hydroxyl radical (HO•), hydrogen peroxide (H<sub>2</sub>O<sub>2</sub>), and superoxide anion radical (O<sub>2</sub><sup>•-</sup>) [4]. These species partake in vascular endothelial cell damage and can lead to membrane lipid peroxidation [4,5]. Moreover, ROS are considered to contribute to the pathogenesis of ALS, a disease characterized by progressive degeneration of upper and lower motor neurons [6]. Free radical-mediated

\* Corresponding author.

E-mail addresses: [velazque@ualberta.ca](mailto:velazque@ualberta.ca) (C.A. Velázquez-Martínez), [siraki@ualberta.ca](mailto:siraki@ualberta.ca) (A.G. Siraki).

<https://doi.org/10.1016/j.freeradbiomed.2019.08.021>

Received 3 March 2019; Received in revised form 13 August 2019; Accepted 20 August 2019

Available online 21 August 2019

0891-5849/ © 2019 Elsevier Inc. All rights reserved.

oxidative stress affects presynaptic transmission, promotes inflammation, and causes lipid peroxidation [6]. Therefore, targeted antioxidant treatments for the restoration of redox balance is an essential consideration in the therapeutic approach.

The free radical scavenging (antioxidant) activity of edaravone is believed to be its mechanism of action, i.e. neuroprotective activity [7]. As edaravone is amphiphilic, it readily crosses biological membranes and distributes to both plasma and tissue, where it may scavenge a wide range of water-soluble and lipid-soluble radicals [7]. Several studies reported that edaravone has potent radical scavenging activity against 2,2-diphenyl-1-picrylhydrazyl (DPPH), HO<sup>•</sup>, tert-butyl peroxy radical, ascorbyl free radical, methyl radical and nitric oxide, although its reactivity with O<sub>2</sub><sup>•-</sup> is controversial [8,9]. Specifically, its therapeutic activity has been attributed to suppressing lipid peroxidation and peroxynitrite-catalyzed cellular damage [7,10]. Under pathological conditions such as (neuro)inflammation, production of peroxynitrite is dramatically increased from the rapid reaction between nitric oxide and O<sub>2</sub><sup>•-</sup> [11]. Fujisawa and Yamamoto reported edaravone to be 30 times more reactive with peroxynitrite compared to uric acid [12].

Although reducing oxidative stress is the postulated mechanism of action of edaravone, the complete picture of its cellular redox regulation is not entirely understood. Myeloperoxidase (MPO) is a heme-containing enzyme abundantly expressed in neutrophils and found to a lesser extent in monocytes [13,14]. Furthermore, some evidence suggests MPO expression in Kupffer cells in the liver, microglia and neuronal cells [15–17]. In response to injury or infection, these cells become activated to release MPO, which can produce highly reactive hypochlorous acid (HOCl) and other oxidants that contribute to microbial killing [18]. Such MPO-derived oxidants can also target proteins, DNA, and lipids to carry out modifications like halogenation, nitration and oxidative cross-linking [19]. Hence, persistent MPO activation and excessive ROS production under pathological conditions could lead to tissue damage and contribute to the pathogenesis of various diseases [19]. A growing body of literature suggests that regulation of the MPO activity is particularly critical when it comes to diseases involving acute or chronic inflammation [20]. Recent clinical and experimental evidence supports the association of MPO in a plethora of pathological conditions such as atherosclerosis, myocardial infarction, cancer, neurodegenerative diseases, glomerulonephritis, ischemia/reperfusion injury and cystic fibrosis, to name a few [16,17,21–30]. Hence modulation of MPO activity to ameliorate the adverse effects has been targeted as a viable therapeutic approach [20].

Directing the MPO redox pathway is essential in modulating the MPO-mediated HOCl production. MPO becomes activated when it reacts with H<sub>2</sub>O<sub>2</sub> to form an active redox intermediate (Compound I). Once produced, Compound I can either enter the chlorination cycle, in which toxic HOCl is produced from chloride ion (Cl<sup>-</sup>), or enter the peroxidase cycle, oxidizing other substrates (electron donors) [19]. Despite the critical contribution of MPO in neuropathology and other diseases, currently, there is no report on the effect of edaravone on MPO activity and MPO-mediated oxidative stress. According to the hypothetical scheme described by Yamamoto et al., edaravone scavenges free radicals by donating one electron to the radical species [7]. As edaravone apparently acts as an efficient electron donor, we postulated that edaravone would serve as a substrate of MPO. In this report, we provide evidence that edaravone acts as an MPO substrate. In addition, we characterized the edaravone free radical as well as edaravone metabolites produced as a result of the MPO-mediated oxidation, followed by evaluation of the cytotoxic potential of the edaravone free radical. Lastly, we describe intriguing findings regarding the concentration-dependent effects of edaravone in both exacerbating and suppressing H<sub>2</sub>O<sub>2</sub>-mediated HL-60 cell toxicity, which we propose to occur via modulation of MPO-mediated HOCl generation.

## 2. Materials and methods

### 2.1. Reagents

Human purified neutrophil MPO was purchased from Athens Research & Technology (Athens, GA). 3-methyl-1-phenyl-2-pyrazolin-5-one (edaravone) and 2-chloro-5,5-dimethyl-1,3-cyclohexanedione (MCD) were purchased from Alfa Aesar (Tewksbury, MA). Diethylenetriamine-pentaacetic acid (DTPA) was purchased from Fluka Analytical (Buchs, Switzerland). Glucose oxidase (GOx), D-(+)-glucose, hydrogen peroxide, L-glutathione reduced, protease inhibitor cocktail, Ponceau S and guaiacol were purchased from Sigma (St. Louis, MO). 5,5-dimethyl-1-pyrroline-N-oxide (DMPO) and Cytotoxicity LDH Assay Kit-WST were purchased from Dojindo Molecular Technologies, Inc. (via Cedarlane Labs, Burlington, ON). Sodium chloride was from VWR (West Chester, PA). CellTiter-Glo<sup>®</sup> Luminescent Cell Viability Assay kit was purchased from Promega (Madison, WI). HL-60 human promyelocytic leukemia cells (#CCL-240) were obtained from ATCC (via Cedarlane Labs, Burlington, ON). Micro BCA<sup>™</sup> Protein Assay Kit was purchased from Thermo Scientific (Rockford, IL). 4X Laemmli Sample Buffer and Transfer-blot<sup>®</sup> semi-dry transfer cell were purchased from Bio-Rad (Hercules, CA). BLUelf Prestained Protein Ladder was from FroggaBio (North York, ON, Canada). Anti-human MPO (rabbit pAb) and Immobilon Western Chemiluminescent HRP Substrate were purchased from EMD Millipore (Billerica, MA). Anti-rabbit IgG, HRP-linked antibody was purchased from Cell Signaling Technology (Whitby, ON, Canada). A stock solution of edaravone (500 mM) was prepared in DMSO and stored at -20 °C up to one month.

### 2.2. UV-Vis spectroscopic analysis of the MPO active site

The effect of edaravone on the catalytic activity of MPO was examined by measuring the kinetic changes in the UV-Vis absorption spectra of the heme active site of the MPO. Reactions of 500 nM MPO with or without 100 μM edaravone was prepared in 0.1 M sodium phosphate buffer (pH 7.4) containing 100 μM DTPA (PB). After initiating the reaction with 100 μM H<sub>2</sub>O<sub>2</sub>, the reaction was allowed to proceed for 1 h. The region of the UV-Vis spectrum spanning the absorption maxima (350–550 nm) of the resting MPO heme (λ<sub>max</sub> = 429 nm) and for MPO Compound II (λ<sub>max</sub> = 456 nm) were measured at t = 0, 2, 5, 10, 20 and 60 min using Thermo Scientific NanoDrop 2000c dual-mode UV-vis spectrophotometer (Wilmington, DE). The absorption spectrum of 500 nM resting MPO in the buffer was recorded as a reference.

### 2.3. UV-Vis spectroscopic analysis of MPO-mediated MCD chlorination

The rate of MPO-catalyzed MCD chlorination into dichlorodimedon (DCD) is an indirect measure of the rate of HOCl production by MPO from H<sub>2</sub>O<sub>2</sub> and Cl<sup>-</sup>. The effect of edaravone on the rate of MPO catalyzed halogenation was investigated using MCD as a chlorination target of HOCl. Reactions were prepared by mixing 50 nM MPO, 200 mM NaCl, 40 μM MCD and different concentrations of edaravone (0, 0.3, 3, 10, 30° and 100 μM), and then initiating the reaction with 300 μM H<sub>2</sub>O<sub>2</sub>. Kinetic changes in the maximum absorption wavelength (λ<sub>max</sub> = 291 nm) of MCD were recorded every 20 s for 100 s. All reactions were carried out in PB. Data were expressed as a change in absorbance at 291 nm from t = 0 (or ΔAbs at 291 nm).

### 2.4. UV-Vis spectroscopic analysis of MPO-catalyzed oxidation of edaravone

Formation of the MPO-catalyzed product of edaravone was detected by measuring kinetic changes in the UV-Vis spectra. 500 nM of MPO and 100 μM of edaravone was mixed, and the reaction was triggered by 100 μM H<sub>2</sub>O<sub>2</sub>, and the UV-Vis spectrum was measured at t = 0, 2, 5, 10,

20 and 60 min to identify the wavelength(s) subject to change. All reactions were carried out in PB. UV–Vis spectra were acquired as described above.

### 2.5. Liquid-chromatography mass-spectroscopy (LC-MS) analysis of edaravone metabolites

Edaravone (500  $\mu$ M) was mixed with 500 nM MPO and 100  $\mu$ M H<sub>2</sub>O<sub>2</sub> in a 200  $\mu$ L reaction mixture using PB. The reaction was carried out for 1 h on a shaker and then stopped by addition of 200  $\mu$ L ice-cold acetonitrile. Reaction components were separated by adding ice-cold acetonitrile to the mixture, followed by vigorous mixing on a vortex for 5 min and then centrifugation at 3000 rpm for 5 min at 4 °C. The organic phase was collected and analyzed by high-resolution LC-MS. RP-HPLC-UV-MS was performed using an Agilent 1200 SL HPLC System with a Phenomenex Kinetex 1.7  $\mu$ m, 100 Å, 50  $\times$  2.1 mm, C8 reverse-phase analytical column with guard (Phenomenex, Torrance, CA, USA), thermostated at 40 °C followed by UV and mass spectrometric detection. An aliquot was loaded onto the column and flushed for 1 min to remove salts at a flow rate of 0.50 mL/min and an initial buffer composition of 99% of 0.1% formic acid as mobile phase A and 1% of 0.1% acetonitrile as mobile phase B. Elution of the analytes was achieved by using a linear gradient from 1% to 99% mobile phase B over a period of 9 min, held at 99% mobile phase B for 1 min to remove all analytes from the column and 99%–1% mobile phase B over a period of 1 min. Mass spectra were acquired in positive mode ionization using an Agilent 6220 Accurate-Mass TOF HPLC/MS system (Santa Clara, CA, USA) equipped with a dual sprayer electrospray ionization source with the second sprayer providing a reference mass solution. Mass spectrometric conditions were drying gas 9 L/min at 325 °C, nebulizer 25 psi, mass range 100–1000 Da, acquisition rate of  $\sim$ 1.03 spectra/sec, fragmentor 150 V, skimmer 65 V, capillary 3800 V, instrument state 4 GHz High Resolution. Mass correction was performed for every individual spectrum using peaks at  $m/z$  121.05087 and 922.00979 from the reference solution. Data acquisition was performed using the Mass Hunter software package (ver. B.04.00). Analysis of the HPLC-UV-MS data was done using the Agilent Mass Hunter Qualitative Analysis software (ver. B.07.00).

### 2.6. Electron spin resonance (ESR) spectroscopy spin-trapping of edaravone and glutathionyl radical

Free radical metabolites of edaravone were detected by ESR spin trapping, where short-lived radical species form covalent adducts with the nitron spin trap agent DMPO to produce a relatively stable paramagnetic species. The reaction mixture consisted of 6.4 mM edaravone, 100 mM DMPO, and 0.5  $\mu$ M MPO, all prepared in PB. The reaction was initiated by a sustained generation of H<sub>2</sub>O<sub>2</sub>, produced from the reaction between 5 mM glucose and 25 mU/mL GOx. After briefly vortexing, the reaction mixture was transferred into three separate 50  $\mu$ L micro-capillary tubes, inserted simultaneously into a 3 mm ESR tube which was then placed in the resonator. ESR spectra were obtained with a Bruker Elexsys E-500 spectrometer (Billerica, MA) with the following parameters: Center field = 3505 G, sweep width = 100 G, Field modulation = 1 G, Microwave frequency = 9.8 GHz, Microwave power = 20 mW, and sweep time = 120 s. Spectra were recorded after two scans. Oxidation of glutathione by edaravone radical into glutathionyl radical was also assessed by ESR spin trapping with DMPO. Reaction mixtures consisted of 100 mM DMPO, 1 mM GSH, and 50 nM MPO in PB were mixed with either 10  $\mu$ M phenol, 10  $\mu$ M edaravone or DMSO (0.02%). After triggering with 100  $\mu$ M H<sub>2</sub>O<sub>2</sub>, ESR spectroscopic analyses were carried out as described above.

### 2.7. NMR studies for exchangeable proton analysis in edaravone

Edaravone (30 mg) was dissolved in 2 mL deuterated DMSO (DMSO-

d<sub>6</sub>; Cambridge Isotopes Laboratories, Tewksbury, MA) for <sup>1</sup>H-NMR spectra acquisition using a Bruker FT-600 MHz NMR spectrometer. <sup>1</sup>H-NMR and <sup>13</sup>C-NMR spectra were determined using tetramethylsilane as a reference. Chemical shifts ( $\delta$ ) and coupling constants ( $J$ ) are expressed in parts per million and Hertz, respectively.

### 2.8. Metabolic activity (ATP) assay of the HL-60 cells

HL-60 human promyelocytic cells were seeded in a 96-well microplate at  $1 \times 10^5$  cells/mL in 100  $\mu$ L phosphate-buffered saline (PBS). Cells were treated with increasing concentration of edaravone (0, 1, 5, 10, 25, 50, 100 and 200  $\mu$ M), then co-stimulated with either a bolus concentration of 30  $\mu$ M H<sub>2</sub>O<sub>2</sub> or 5 mM glucose and 10 mU/mL GOx to induce toxicity. Cells receiving no treatment and 0.04% DMSO treatment were included as a negative control (NC) and vehicle control, respectively. Following 3 h incubation, CellTiter-Glo<sup>®</sup> Luminescent Cell Viability Assay was performed following the manufacturer's instruction. Luminescence values were presented as a percentage of the vehicle control and expressed as mean  $\pm$  SD. All treatments were carried out in triplicates, and the assay was repeated three independent times. Statistical analysis was carried out by one-way ANOVA with Bonferroni multiple comparisons ( $n = 3$ ) using GraphPad Prism 6 software.

### 2.9. Cytotoxicity (LDH) assay of the HL-60 cells

HL-60 cells were treated with edaravone and H<sub>2</sub>O<sub>2</sub> as described above. The LDH activity assay was carried out according to the manufacturer's instruction. Briefly, 10  $\mu$ L of lysis buffer was added to the untreated cells for the last 30 min of incubation to establish 100% cytotoxicity (positive control, PC). Similarly, cells in other wells were treated with PBS (negative control, NC), and vehicle control (DMSO). The dye mixture in assay buffer (100  $\mu$ L) was added to each well and incubated in the dark for 30 min. Stop solution (50  $\mu$ L) was added, and the absorbance was recorded at 490 nm. The percent cytotoxicity was calculated using the following formula:

$$[\text{Cytotoxicity (\%)} = (A_{\text{Test substance}} - A_{\text{PC}}) / (A_{\text{PC}} - A_{\text{NC}})]$$

The percent cytotoxicity was expressed as mean  $\pm$  SD. Statistical analysis was carried out by one-way ANOVA with Bonferroni multiple comparisons ( $n = 3$ ) using GraphPad Prism 6 software.

Data were normalized as the percentage of negative control and positive control for CellTiter-Glo and LDH assay, respectively.

### 2.10. Western blot analysis of MPO amount in HL-60 cells

HL-60 total cell protein lysates were prepared using RIPA buffer (1% Triton X-100, 0.5% Sodium deoxycholate, and 0.1% SDS in PBS pH 7.4) containing protease inhibitor cocktail (10  $\mu$ L per  $10^7$  cells), followed by three freeze-thaw cycles. Mixtures were centrifuged at 15,000 rpm for 15 min at 4 °C, and the supernatant was collected. Human purified MPO (0.3, 1, 3 and 9  $\mu$ g) and the HL-60 total cell protein lysate (containing 0.1, 0.3 and  $0.9 \times 10^6$  cells) were reconstituted in 4X Laemmli buffer and subjected onto the same gel for electrophoretic separation, followed by semi-dry transfer onto nitrocellulose membranes. Membranes were blocked with blocking buffer consisting of 5% non-fat skim milk in Tris-buffered saline with 0.1% Tween-20 (TBST) for 1 h at room temperature and incubated overnight at 4 °C with primary anti-MPO Rabbit pAb (1:4000) in blocking buffer. The secondary goat anti-rabbit IgG, HRP-linked antibody (1:5000) was incubated for 1 h at room temperature. Membranes were washed three times with TBST after each step of immunoblotting. Immunoblots were visualized with Immobilon Western Chemiluminescent HRP Substrate using ImageQuant LAS 4000mini Luminescent image analyzer (GE Healthcare, Pittsburgh, PA). Band intensities were quantified using ImageJ software (NIH, United States) and expressed as mean  $\pm$  SD

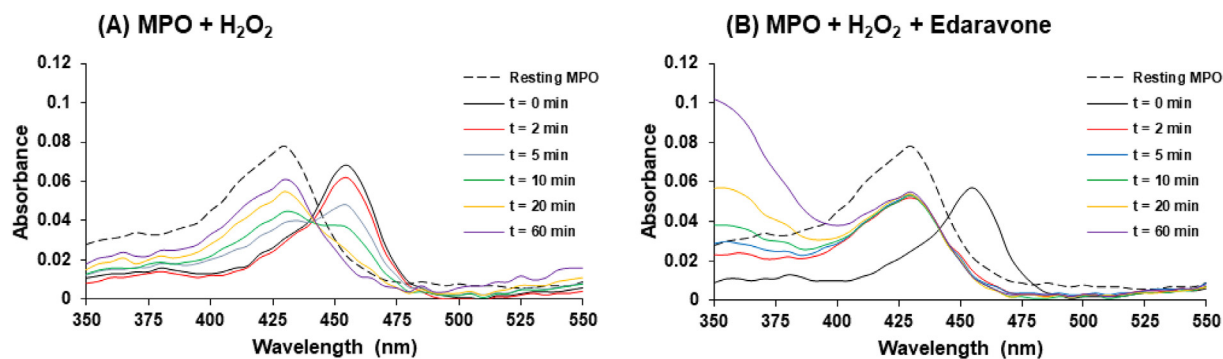


**Fig. 1.** Effect of edaravone on reducing MPO to its resting state. The reaction of 500 nM MPO in the absence (A) or presence (B) of 100  $\mu\text{M}$  edaravone was prepared in 0.1 M sodium phosphate buffer (pH 7.4) containing 100  $\mu\text{M}$  DTPA (PB). After triggering the reaction with 100  $\mu\text{M}$   $\text{H}_2\text{O}_2$ , UV-Vis spectra were acquired at  $t = 0, 2, 5, 10, 20$  and 60 min. Absorption peaks in the Soret region show native MPO ( $\lambda_{\text{max}} = 429 \text{ nm}$ ) and MPO Compound II ( $\lambda_{\text{max}} = 456 \text{ nm}$ ).

( $n = 3$ ).

### 3. Results

#### 3.1. The effect of edaravone on the rate of MPO regeneration

Kinetic UV-Vis spectroscopy studies in a reaction containing 500 nM MPO and 100  $\mu\text{M}$   $\text{H}_2\text{O}_2$  revealed the rapid formation of Compound II at  $\lambda_{\text{max}} = 456 \text{ nm}$ . Regeneration of native MPO ( $\lambda_{\text{max}} = 429 \text{ nm}$ ) from MPO Compound II occurred slowly over 60 min, which is typical in the absence of a donor substrate (Fig. 1A) [31]. When 500  $\mu\text{M}$  of edaravone was added to the full reaction, the initial formation of the Compound II was observed but rapidly regenerated to native MPO within 2 min, significantly increasing the rate of MPO peroxidase cycle (Fig. 1B). These data demonstrate that edaravone acts as an efficient electron donor substrate for the MPO peroxidase activity.

#### 3.2. The effect of edaravone on MPO-mediated HOCl formation (chlorination of MCD)

Chloride ion is readily oxidized to HOCl by the MPO Compound I. Chlorination of MCD into DCD by HOCl was used as a surrogate marker of HOCl production from MPO/ $\text{H}_2\text{O}_2$  reaction [32]. The absorbance maximum of MCD at 291 nm decreases upon chlorination into DCD. The change in absorbance of MCD at each time point from the  $t = 0$  reflects the extent of MCD chlorination, and with time, the relative rate of HOCl produced. In a reaction with 50 nM MPO, 200 mM NaCl and 300  $\mu\text{M}$   $\text{H}_2\text{O}_2$ , MCD was chlorinated at a constant rate over 100 s. Introduction of 0.3, 3 and 10  $\mu\text{M}$  of edaravone to the reaction concentration-dependently augmented the MPO-mediated chlorination of

MCD (Fig. 2A). Interestingly, 30  $\mu\text{M}$  of edaravone resulted in diminished MCD chlorination, which was further pronounced at 100  $\mu\text{M}$  edaravone (Fig. 2B). Therefore, our results indicate that under the given conditions, 0.3–10  $\mu\text{M}$  edaravone increased the rate of MCD chlorination (HOCl production), whereas 30 and 100  $\mu\text{M}$  attenuated the rate of HOCl production.

#### 3.3. MPO peroxidase activity catalyzes UV-Vis spectral changes of edaravone

The data presented thus far revealed a role for edaravone in the MPO activity. Kinetic UV-Vis analysis was performed to confirm that the peroxidase activity of MPO catalyzed edaravone into its corresponding metabolite(s) (Fig. 3). The UV-Vis spectra of the reaction between 100  $\mu\text{M}$  edaravone and 500 nM MPO/100  $\mu\text{M}$   $\text{H}_2\text{O}_2$  were monitored for 60 min. Examination of the entire UV-Vis spectrum detected a significant increase in absorbance at 350 nm by 10.3-fold after 60 min compared to  $t = 0$  (Fig. 3). The increased absorption at this wavelength is expected to correspond to the MPO-oxidized metabolite (s) of edaravone. No other significant metabolite was detected by the UV-Vis spectroscopy.

#### 3.4. Metabolite formation by MPO-mediated oxidation of edaravone

To further characterize the MPO-mediated oxidation of edaravone, the reaction mixture of MPO/ $\text{H}_2\text{O}_2$ /edaravone was analyzed by LC-MS. The total ion current (TIC) scan was used to acquire the retention time for metabolites and provide  $m/z$  by high-resolution MS. We were not able to propose structures for all metabolites, but certain major ones previously reported to occur through oxidation of edaravone were

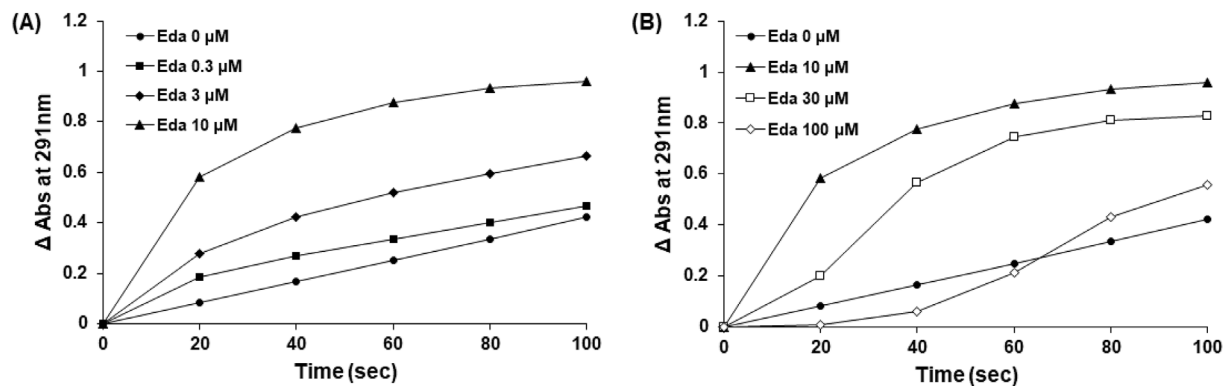


**Fig. 2.** Concentration-dependent effect of edaravone on the MPO-mediated chlorination of MCD. Each 300  $\mu\text{L}$  of reaction in PB contained 50 nM MPO, 200 mM NaCl, 40  $\mu\text{M}$  MCD with 0, 0.3, 3, 10 (A), 0, 10, 30 or 100  $\mu\text{M}$  (B) of edaravone. Following the addition of 300  $\mu\text{M}$   $\text{H}_2\text{O}_2$ , absorbance at 291 nm was measured every 20 s for 100 s. The change in the absorbance was obtained by subtracting the absorbance at  $t = 0$  from each measured time point.

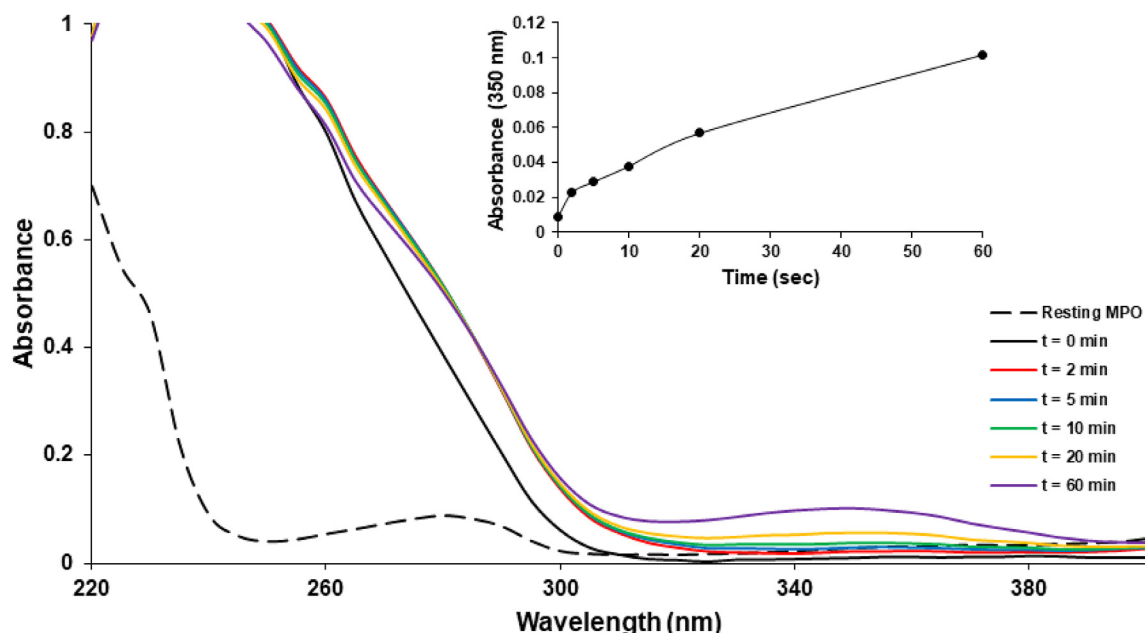


**Fig. 3. Accumulation of MPO-catalyzed edaravone product(s) detected by UV-Vis spectroscopy.** A reaction of 500 nM and 100  $\mu\text{M}$  edaravone was prepared in PB. After triggering the reaction with 100  $\mu\text{M}$   $\text{H}_2\text{O}_2$ , UV-Vis spectra were recorded at  $t = 0, 2, 5, 10, 20$  and 60 min. The figure inset shows the formation of the edaravone product over 60 min at 350 nm. An absorption spectrum of 500 nM resting MPO in the PB was recorded as a reference.

referred to for guidance [7,10].

The  $m/z$  for (2) appeared to elute multiple times (3.97, 5.40, 5.56); it is possible that this is due to an isomer having the same elemental composition. The latter is possible as structures in (4) and (5) are proposed to be a trimer and tetramer of edaravone that necessitates bond formation between the phenyl rings. The retention times, formulas,  $m/z$  and calculated  $m/z$  are shown in Table 1, and the extracted ion chromatograms along with proposed structures as determined using high-resolution LC-MS are shown in Fig. 4.

### 3.5. MPO-catalyzed edaravone radical is detected by ESR spin trapping with DMPO

In Fig. 5, we have shown a free radical trapped during MPO-catalyzed oxidation of edaravone using DMPO spin trapping with ESR spectroscopy. The DMPO/ $\bullet$ edaravone adduct produced a six-line spectrum indicative of a carbon-centred edaravone radical (Fig. 5A). The signal intensity significantly diminished when GOx (the  $\text{H}_2\text{O}_2$  source) was removed from the system (Fig. 5B). The DMPO/ $\bullet$ edaravone signal was not detected if MPO was omitted from the complete system (Fig. 5C). A simulated spectrum of the experimental spectrum in Fig. 5A is shown in Fig. 5D. The simulation revealed an unprecedentedly large hyperfine splitting constant. In order to validate the simulated and experimental findings, we calculated the dihedral angle between the C–H bond and nitrogen  $\pi$ -orbital electrons by the following equation [33]:

$$\alpha_{\beta}^H = (B_0 + B\cos^2\theta)\rho_N$$

**Table 1**  
Chromatographic details for edaravone metabolites.

Name	RT	Formula	$m/z$	Calc. $m/z$ (exact mass + $\text{H}^+$ )	$\Delta$ (ppm)
Edaravone	3.41	$\text{C}_{10}\text{H}_{10}\text{N}_2\text{O}$	175.0868	175.0866	–1.2
(2)	3.97, 5.40, 5.56	$\text{C}_{20}\text{H}_{18}\text{N}_4\text{O}_2$	347.1503	347.1503	–0.14
(3)	4.92	$\text{C}_{20}\text{H}_{18}\text{N}_4\text{O}_3$	363.1443	363.1452	2.39
(4)	5.48	$\text{C}_{30}\text{H}_{26}\text{N}_6\text{O}_3$	519.2125	519.2144	2.73
(5)	5.96	$\text{C}_{40}\text{H}_{34}\text{N}_8\text{O}_4$	691.2754	691.2781	3.15

where  $\theta$  is the dihedral angle,  $\rho_N$  is the spin density on the nitrogen atom of the nitroxyl function,  $B$  is the proportionality constant for each radical adduct, and  $B_0$  is the same constant when  $\theta = 90^\circ$ . For nitroxides,  $B_0 \approx 0$ ,  $\rho_N \approx 0.5$ . For the spectrum observed with edaravone,  $\alpha_{\beta}^H = 28.1 \text{ G}$ , and  $B = 62 \text{ G}$ , therefore  $\theta \approx 18^\circ$ . If the same calculation was applied to a much smaller free radical trapped by DMPO (i.e., hydroxyl radical), the result is  $\theta \approx 36^\circ$ . These calculations and findings are in agreement with observations reported by Janzen et al., 1985<sup>33</sup>, where large free radical molecules would produce a small dihedral angle.

### 3.6. Proton exchange to determine the site of ionization on edaravone

Using  $d_6$ -DMSO, studies were carried out to determine if the hydrogens on the  $\alpha$ -carbon (adjacent to the carbonyl) were exchangeable with deuterium oxide (Fig. 6). Edaravone in DMSO- $d_6$  was present in the enol form (Fig. 6A), with the following proton splittings:  $\delta$  11.47 (s, 1H), 7.75–7.70 (m, 2H), 7.44–7.38 (m, 2H), 7.22–7.17 (m, 1H), 5.35 (s, 1H), 2.12 (s, 3H). Upon addition of  $\text{D}_2\text{O}$ , the hydrogens on the  $\alpha$ -carbon and the enol both exchanged with  $^2\text{D}$  (Fig. 6B).

### 3.7. Edaravone radical-induced glutathionyl radical formation

The potency of edaravone radical to oxidize glutathione was assessed by ESR spin trapping using DMPO. The edaravone radical produced from the reaction of 50 nM MPO/100  $\mu\text{M}$   $\text{H}_2\text{O}_2$  oxidized glutathione into glutathionyl radical, which was trapped using DMPO to produce a characteristic four-line spectrum corresponding to the DMPO/ $\bullet$ SG (Fig. 7a). However, the intensity of the spectrum was minor

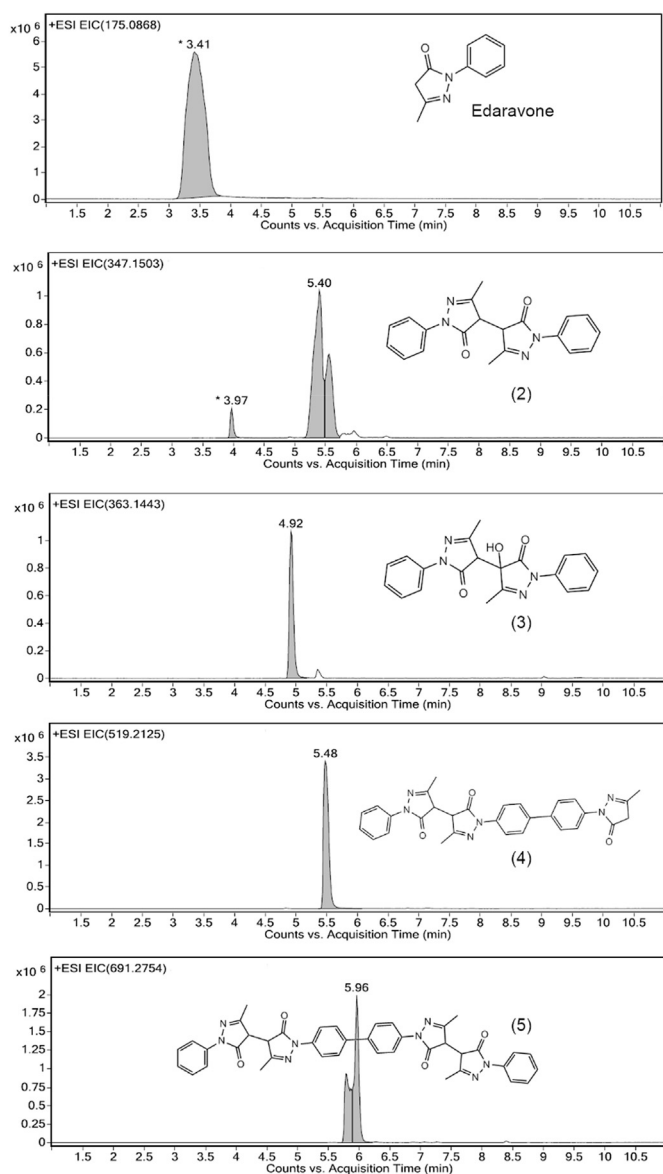


**Fig. 4.** High-resolution LC-MS analysis of MPO-catalyzed oxidation products of edaravone. The reaction mixture consisted of 500  $\mu\text{M}$  edaravone, 500 nM MPO and 100  $\mu\text{M}$   $\text{H}_2\text{O}_2$  was incubated for 1 h. Edaravone (1) and its MPO-catalyzed metabolites (2, 3, 4 and 5) were analyzed after liquid-liquid extraction. For clarity, we have shown the extracted ion chromatograms for each specific metabolite due to the overlapping retention times for some of the metabolites.

compared to the vehicle control (Fig. 7c) and was significantly less intense compared to the DMPO/ $\bullet\text{SG}$  produce by phenoxy radicals (Fig. 7b).

### 3.8. Edaravone exhibits a concentration-dependent biphasic effect on $\text{H}_2\text{O}_2$ -induced toxicity of HL-60 cells

Human acute promyelocytic leukemia (HL-60) cells constitutively express a high level of MPO. Cell viability (metabolic activity using CellTiter-Glo™) and cytotoxicity (LDH assay) were performed to examine the effect of edaravone on  $\text{H}_2\text{O}_2$ -induced toxicity of HL-60 cells (Fig. 8). A bolus concentration of 30  $\mu\text{M}$   $\text{H}_2\text{O}_2$  (Fig. 8A) and a flux of  $\text{H}_2\text{O}_2$  produced by glucose/GOx (G/GOx) (Fig. 8B) induced a significant decrease in cell viability (drop in ATP) over 3 h. The 100 and 200  $\mu\text{M}$  of edaravone dose-dependently protected against the  $\text{H}_2\text{O}_2$ -induced

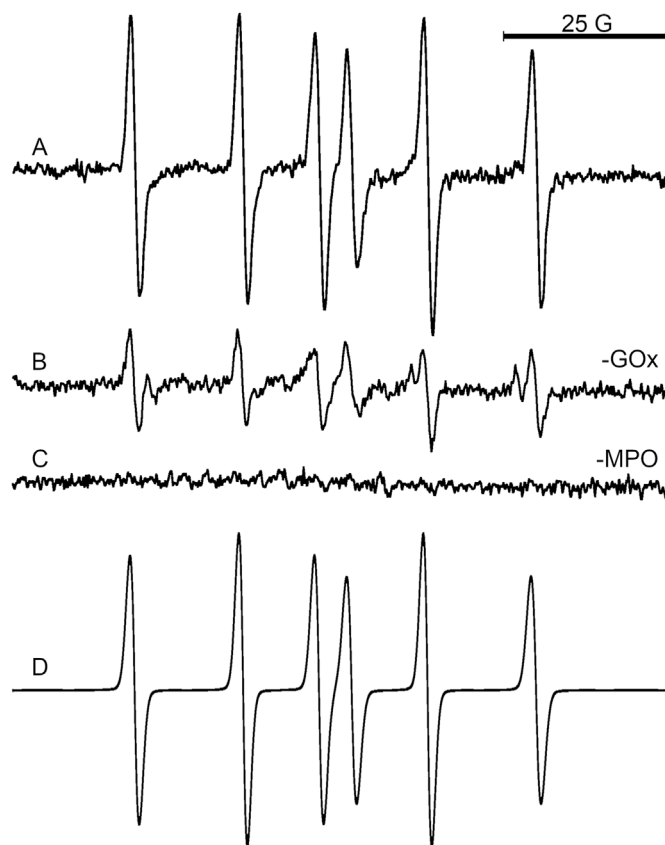


**Fig. 5.** Formation of the edaravone free radical metabolite through peroxidase activity of MPO analyzed by ESR. (A) The experimental spectrum run with PB consisted of 6.4 mM edaravone, 100 mM DMPO, 500 nM MPO, 5 mM glucose and 25 mU/mL glucose oxidase (GOx). (B) GOx and (C) MPO were removed from the complete system, respectively in the control reactions. ESR spectra were acquired by transferring the reaction into 3 separate 50  $\mu\text{L}$  microcapillary tubes, inserted simultaneously into a 3 mm ESR tube which was then placed in the resonator. ESR spectrometer settings: Center field = 3505 G, sweep width = 100 G, Field modulation = 1 G, Microwave frequency = 9.8 GHz, Microwave power = 20 mW, sweep time = 120 s, number of scans = 2. (D) The simulated spectrum was well correlated to the experimental spectrum ( $r = 0.99$ , produced using Winsim 2002), where the  $a^{\text{N}} = 16.5$  G and  $a^{\text{H}} = 28.1$  G.

decrease in ATP and the increase in cytotoxicity; conversely, the addition of 1–10  $\mu\text{M}$  of edaravone exacerbated the  $\text{H}_2\text{O}_2$ -induced cytotoxicity in G/GOx-treated cells, and appeared to do the same in  $\text{H}_2\text{O}_2$ -treated cells, but the latter was not statistically significant. The concentration-dependent biphasic toxic-protective effect of edaravone on  $\text{H}_2\text{O}_2$ -induced toxicity was reproduced in the LDH assay (Fig. 8C). A bolus concentration of 30  $\mu\text{M}$   $\text{H}_2\text{O}_2$  induced significant cytotoxicity, which was significantly augmented by the addition of 1 and 5  $\mu\text{M}$  of edaravone, whereas 25–100  $\mu\text{M}$  of edaravone provided reversal of the  $\text{H}_2\text{O}_2$ -induced toxicity. The LDH assay was not conducted for G/GOx-treated cells due to colorimetric interference (data not shown).

### 3.9. MPO estimation in HL-60

Cellular MPO protein content was approximated by immunoblotting the purified human MPO and the HL-60 cell total protein lysate (Fig. 9). The band intensities for the purified MPO increased linearly with the concentration (0.33, 1, 3 and 9  $\mu\text{M}$ ). Based on a calibration curve, the amount of MPO in  $10^6$  HL-60 cells was estimated to be 11.5  $\mu\text{g}$ . This estimation was performed based on the intensities of the MPO heavy subunit (55 kDa).

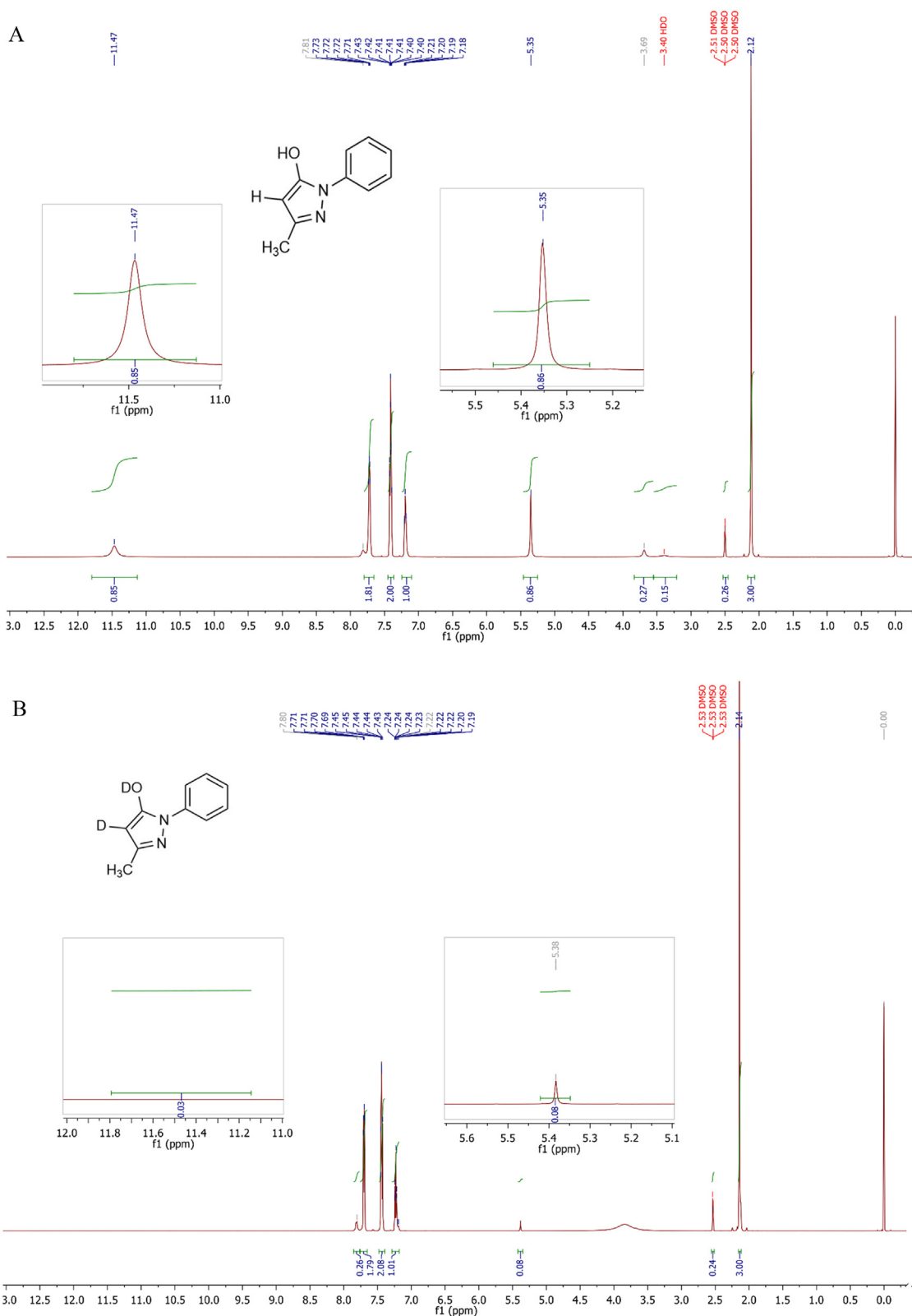


**Figure 6.** 600 MHz  $^1\text{H-NMR}$  spectrum of edaravone in  $\text{DMSO-d}_6$  with the subsequent addition of  $\text{D}_2\text{O}$ . Edaravone in  $\text{DMSO-d}_6$  appeared to be in the keto form (A), but after addition of  $\text{D}_2\text{O}$ , the spectrum demonstrated that the hydrogens (on the enol and the  $\alpha$ -carbon) exchanged with deuterium (B).

#### 4. Discussion

Edaravone has received much attention in the last few years as the first ALS treatment option in over two decades to receive approval from

the U.S. Food and Drug Administration, in addition to the existing oral drug riluzole [1,34]. Since 2015, Mitsubishi Tanabe Pharma Corporation has also gained marketing approval for edaravone in Japan, South Korea, the United States and Canada [1,2,35].

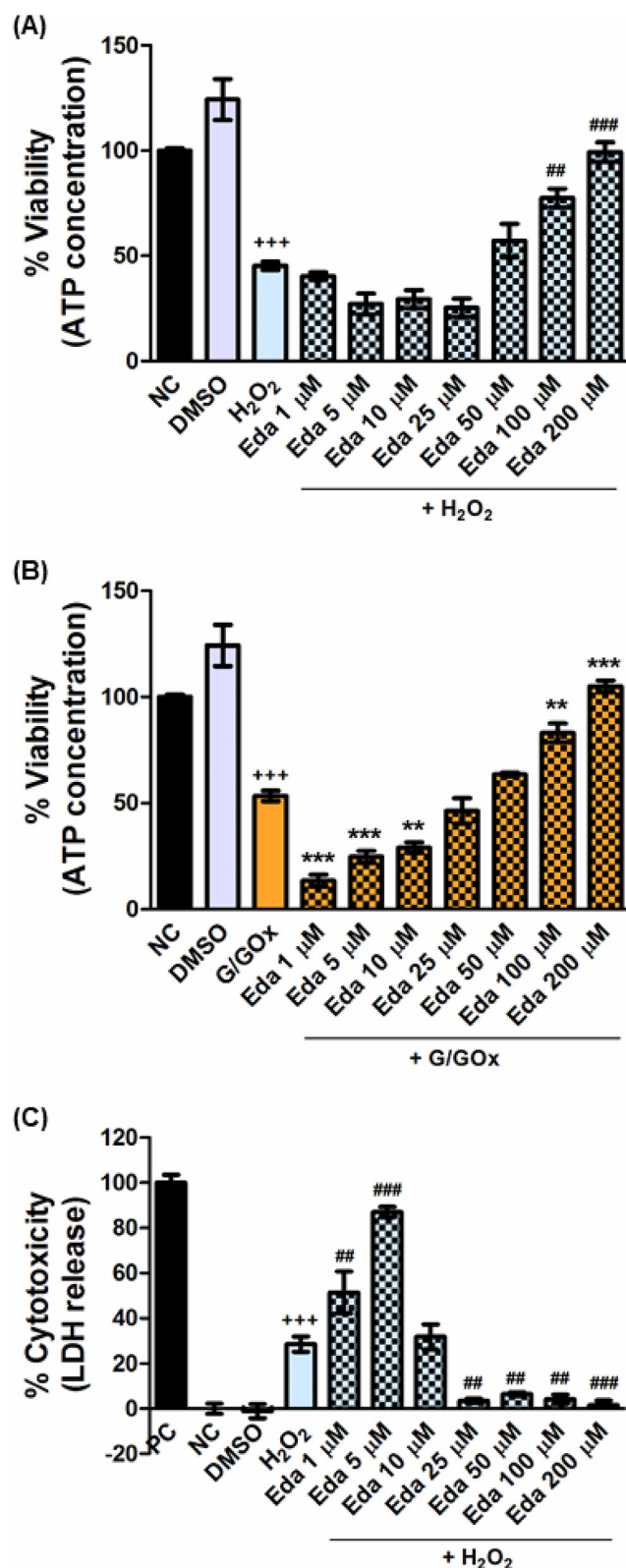


**Fig. 7. Glutathionyl radical detection produced by edaravone or phenol oxidation by MPO/H<sub>2</sub>O<sub>2</sub>.** The characteristic four-line spectra correspond to the DMPO/•SG spin adduct. Reactions were carried out in PB, which contained 100 mM DMPO, 1 mM GSH, 50 nM MPO, and 10 μM edaravone (a), 10 μM phenol (b), or DMSO (vehicle control, c). Reactions were initiated by the addition of 100 μM H<sub>2</sub>O<sub>2</sub>, vortexed briefly, then transferred to 3 × 50 μL microcapillary tubes which were placed in an ESR tube for acquiring spectra. ESR parameters were the same as described previously, except one scan was performed.

Although a considerable amount of work has been conducted to establish the antioxidant properties of edaravone, it remains controversial whether its pharmacological effects can be ascribed entirely to free radical scavenging. Pathobiology of a wide range of diseases involve influx of neutrophils to the site of injury, which release ROS and exacerbate local oxidative damage, inflammation and consequent tissue injury [36]. As a potent antioxidant drug, numerous studies provide evidence that edaravone is a good candidate for treating diseases involving oxidative stress for its protective effects, including the reduced neutrophil infiltration to the site of injury. Yang et al. have shown that edaravone provided significant protective effects against neutrophil infiltration and tissue injury in acute pancreatitis and associated lung injury in rats [37]. In an acute liver injury model induced by co-administration of D-galactosamine and lipopolysaccharide, edaravone reduced neutrophil infiltration to the rat liver tissues, and attenuated the oxidative stress and inflammation [38]. However, the direct effect of edaravone on MPO activity in neutrophils has not yet been elucidated to our knowledge. The present study illustrates a new activity of edaravone by demonstrating its role in modulating the MPO-mediated oxidative stress.

Mounting evidence points toward MPO as a critical contributing player in the progression and pathogenesis of various diseases, especially those characterized by acute or chronic inflammation [19]. Excessive generation of oxidants by MPO has been correlated with tissue damage in neurodegenerative, cardiovascular, renal, lung, and other chronic inflammatory diseases [19]. Much of the MPO-mediated oxidative stress is caused by HOCl (or other hypohalous acids) [39]. The short-lived and highly reactive HOCl targets a wide range of cellular biomolecules exerting cytotoxic effect [40]. Oxidation of cysteine residues by HOCl can affect the functions of critical transcriptional factors and regulatory proteins that contain cysteine in their active site [40]. HOCl can also chlorinate amines and amides in phospholipids, glycosaminoglycan, DNA and RNA [40]. These reactions result in the formation of long-lived chloramines, some of which retain oxidizing activities and contribute to prolonged tissue damage [41,42]. Oxidation of glutathione by HOCl further disrupts the cellular redox balance, exacerbating the oxidative damage and kindling inflammatory processes [40]. Moreover, HOCl acts as a precursor to other reactive species such as HO•, singlet oxygen (<sup>1</sup>O<sub>2</sub>) and ozone (O<sub>3</sub>) [43–45]. Therefore, an MPO inhibitor that interferes with pathologically persistent activation of MPO has been considered a viable target for therapeutic intervention. For example, AZD5904 is a new compound being developed (Phase 1 studies have been completed) as a clinical inhibitor of MPO based on 2-thioxanthines [46,47].

Production of HOCl depends on the competition between the two competing MPO redox pathways (i.e., chlorination vs. peroxidation). The active heme center of MPO exists in multiple redox intermediates



(caption on next page)

depending on its oxidation status. The resting enzyme is in its ferric form [MPO-Fe(III)] and is converted to Compound I containing oxyferryl [MPO-Fe(IV)=O] heme center upon reacting with H<sub>2</sub>O<sub>2</sub>. In the halogenation cycle, halides and pseudo-halides directly reduce Compound I back to its resting state. This cycle produces reactive hypohalous acids (HOCl, HOBr) or hypothiocyanate. Alternatively,

**Fig. 8. Concentration-dependent effect of edaravone on H<sub>2</sub>O<sub>2</sub>-induced cytotoxicity of HL-60 cells.** HL-60 cells were treated with a bolus concentration of 30 μM H<sub>2</sub>O<sub>2</sub> (A and C) or 5 mM glucose (G) and 10 mU/mL GOx (B) for 3 h in PBS with or without 1, 5, 10, 25, 50, 100 and 200 μM of edaravone (Eda). Cell viability (ATP) and cytotoxicity (LDH) were assessed by CellTiter-Glo (A and B) and LDH (C), respectively. Data were analyzed by One-way ANOVA with Bonferroni multiple comparisons (n = 3). The results represent the mean values ± SD. Statistically significant comparisons: +++ p < 0.001 compared to the negative control (NC); \*\*p < 0.01 and \*\*\*p < 0.001 compared to H<sub>2</sub>O<sub>2</sub>; \*\*p < 0.01 and \*\*\*p < 0.001 compared to G/GOx. NC, negative control (PBS); PC, positive control (lysis buffer); DMSO, 0.04% DMSO solvent control; Eda, edaravone.

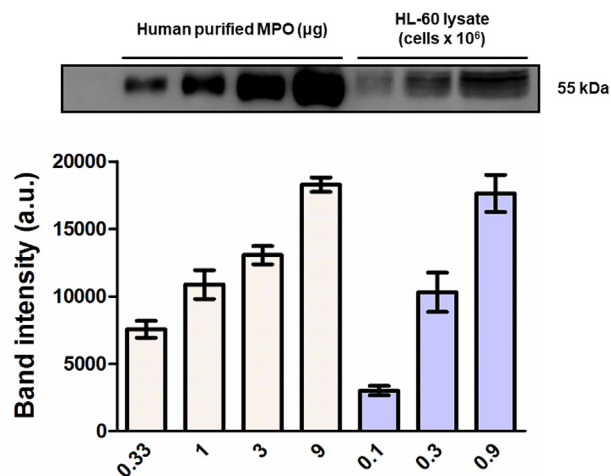


**Fig. 9. Intracellular MPO content in HL-60 cells compared to isolated MPO.** Human purified MPO (0.33, 1, 3 and 9 μg) and the HL-60 cell total protein lysate (0.1, 0.3 and 0.9 × 10<sup>6</sup> cells) were subjected to western blot analysis. Band intensities for the MPO heavy chain subunit (55 kDa) were quantified using ImageJ. Data is presented as mean ± SD (n = 3).

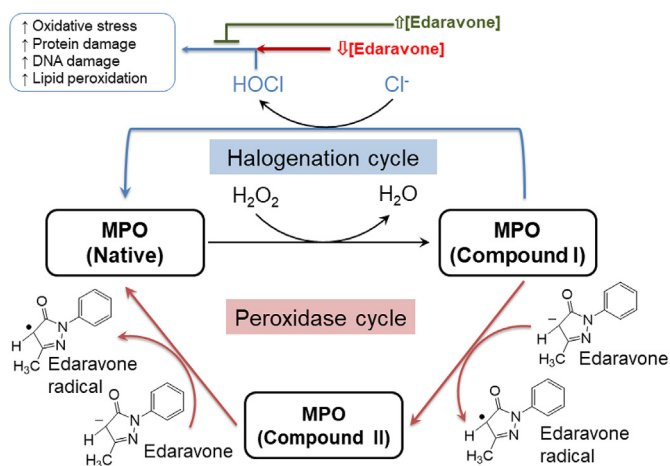


**Fig. 10. The role of edaravone in modulating the MPO catalytic cycles.** At physiological concentration, the chloride ion is a potential substrate for oxidation by MPO Compound I and hypochlorous acid is the major product. Edaravone serves as a peroxidase substrate, enhancing the rate of Compound II reduction and native MPO regeneration. Edaravone is oxidized by Compound I/II to a free radical metabolite. We propose that the halogenation cycle is pronounced when edaravone concentrations are low (up to 10 μM in this study). On the other hand, the non-HOCl producing peroxidase cycle is favoured when the edaravone concentration is high (≥ 30 μM in this study).

Compound I may also oxidize substrates in two sequential one-electron oxidation steps through the formation of another redox intermediate Compound II (MPO-Fe(IV)-OH). Compound I can either follow the

halogenation cycle or the peroxidase cycle depending on the apparent bimolecular rate constant and donor concentrations [40,48]. Kinetic UV-Vis analyses revealed edaravone plays a role in the cycling of MPO redox intermediates by serving as a peroxidase substrate of MPO, as evident by its effect on Compound II reduction back to the resting state. This efficient enzymatic turnover, however, may play a role in the enhancement of HOCl formation, as evidenced by MCD chlorination. These data collectively suggest that edaravone at low concentration (0.3–10 μM) enhanced the resting MPO regeneration through the peroxidase cycle, increasing the rate of Compound I formation that reacts with Cl<sup>-</sup> to produce HOCl. It is likely that a relatively higher concentration of MCD (40 μM) continuously consumed HOCl from the system, shifting the reaction equilibrium towards the HOCl production. In contrast, the rate of HOCl production concentration-dependently decreased when edaravone concentrations were increased to 30 μM and above. This observation can be explained by the HOCl-producing halogenation cycle being outcompeted by the introduction of a high concentration of edaravone as the MPO substrate and target for HOCl. Moreover, as the peroxidase pathway becomes dominant under high donor (edaravone) concentrations, the amount of Compound I available to undergo the halogenation pathway decreases. Therefore, a low concentration of edaravone can enhance the halogenation activity and the HOCl production in the MPO/H<sub>2</sub>O<sub>2</sub>/Cl<sup>-</sup> system, whereas a high concentration of edaravone divert the enzymatic activity towards the peroxidase cycle and reduce HOCl production.

MPO-catalyzed metabolites of edaravone were analyzed and compared to previously reported findings from edaravone oxidation by free radicals. Yamamoto et al. described the time-course formation of the oxidation products of edaravone [7]. Initially, edaravone anion is thought to donate an electron to a radical, converting the radical to the corresponding anion [7]. The resulting edaravone radical is converted to edaravone peroxy radical by reacting with oxygen [7]. Subsequent formation of 4-oxoedaravone was observed as the main product, along with small amounts of a hydroxylated edaravone dimer (BPOH) [7]. The 4-oxoedaravone was hydrolyzed into 2-oxo-3-(phenylhydrazono) butanoic acid [7].

In our experiment, the time-dependent formation of the MPO-catalyzed metabolites was confirmed by kinetic UV-Vis spectroscopy. The product formed at λ<sub>max</sub> of 350 nm could be the same product reported at λ<sub>max</sub> of 345 nm formed by peroxy and azidyl radicals [49]. Several different metabolite structures of edaravone were detected by LC-MS. In contrast to earlier findings, we did not find species that corresponded to 4-oxoedaravone or its hydrolyzed product. However, we detected a structure corresponding to BPOH, and a molecule structurally similar to the BPOH only without the 4-hydroxyl group. Interestingly, dimers, trimers, and tetramers of edaravone were also detected. We detected a trace amount of dimer present in the starting material (data not shown), though this may not be sufficient to partake in radical dimerization.

As we demonstrated in this study that edaravone serves as a peroxidase substrate of MPO, a free radical intermediate was hypothesized to be produced during the peroxidase cycle of MPO. ESR spin-trapping with DMPO revealed the formation of a primary edaravone radical through MPO-mediated oxidation. The stability of the edaravone radical was previously investigated by Ono et al. [50]. Based on the electron density function calculation, they concluded the unpaired electron on the pyrazoline radical was highly delocalized, and thus its reactivity should be much less than that of reactive oxygen radicals such as HO•, alkyl peroxy radicals, and alkoxy radicals [50]. However, our findings conclusively demonstrated that a carbon-centred radical was formed and trapped. To further validate the formation of a carbon-centred free radical, we performed NMR studies to determine proton exchange using D<sub>2</sub>O. Our findings indicated that the α-carbon could be ionized, and its proximity to the carbonyl group likely facilitates its ionization (pK<sub>a</sub> = 6.9) [51]. An extreme example of this is phenylbutazone, which has an acidic carbon between two ketone groups (pK<sub>a</sub> = 4.5) [52]. The antioxidant activity of edaravone (and

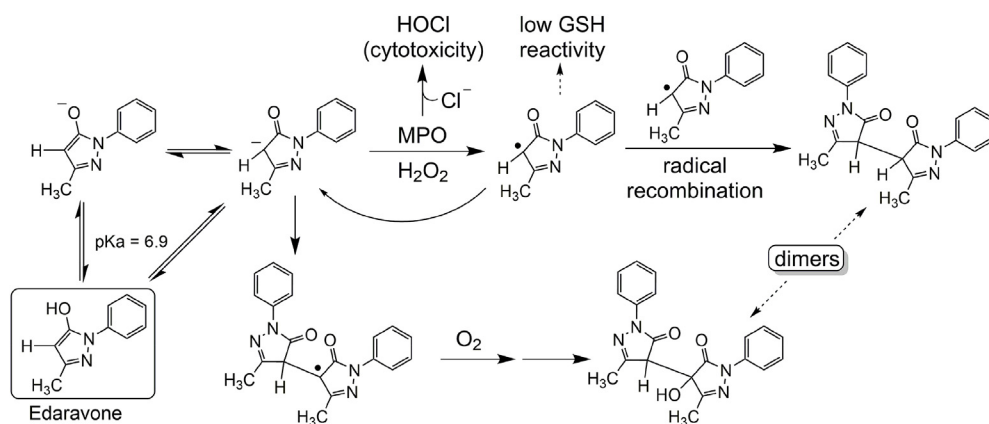


**Fig. 11. Proposed mechanisms of MPO-mediated oxidation of edaravone based on observations in this study.** Edaravone undergoes keto-enol tautomerization as well as ionization. The carbanion-keto form of edaravone is shown for simplicity, which is apparently detected as dimer structures using LC-MS (i.e., the enol is no longer detected after MPO oxidation). The carbon-centred radical of edaravone was verified by ESR spin trapping with DMPO, and some of the dimer products previously reported were verified using LC-MS in this study, in addition to new proposed metabolites [10].

thus its ionization potential) has been ascribed in part to its ionization which facilitates electron transfer [53]. To investigate the relative oxidizing potential of the edaravone radical, we tested its ability to oxidize glutathione in comparison to the highly reactive phenoxyl radical using ESR spin-trapping of the glutathionyl radical with DMPO. In agreement with the finding of Ono et al., 1997, edaravone radical showed only a minor reactivity with glutathione compared to control and significantly less than that of phenoxyl radical [41].

In order to evaluate the intracellular effects of edaravone,  $H_2O_2$ -treated HL-60 cells (abundant in MPO) were assessed for cell viability. Interestingly, edaravone exacerbated the  $H_2O_2$ -induced toxicity at a low concentration range while attenuating it at a high concentration range. This observation correlates with the concentration-dependent biphasic effect of edaravone on the rate of HOCl production, as this phenomenon cannot be explained by the free radical scavenging activity of edaravone alone.

The cell viability assay assumes the cell count based on the ATP quantitation [54], and the LDH assay result verifies that  $H_2O_2$  indeed induced cell death via membrane lysis. Many studies have demonstrated that  $H_2O_2$ -induced apoptotic and necrotic death in HL-60 cells is dependent on the HOCl generation with subsequent formation of chloramines by reaction with amines and amides [55,56]. Although there is no strict consensus on the exact concentration, there is a threshold concentration of HOCl, above which the majority of cell death is manifested by necrosis rather than apoptosis [57]. For example, Wagner et al. has demonstrated that 10–15  $\mu M$  of  $H_2O_2$  induces apoptosis in HL-60 cells, and necrosis at concentrations > 20  $\mu M$  based on the DNA fragmentation assay. Under our experimental conditions, 30  $\mu M$   $H_2O_2$  induced significant cell death in HL-60 cells, which was increased or decreased depending on the edaravone concentration, although the mechanism of cell death was not clarified as it is beyond the scope of the current study.

Lastly, MPO content in HL-60 total cell protein lysate was estimated. Surprisingly, the MPO amount we found by immunoblotting was higher than what was previously reported [58]. Firstly, small-scale purification poses significant variation in protein content during the processing. In addition, MPO is a multimeric protein composed of two heavy subunits (55 kDa) and two light subunits (15 kDa) which are denatured into several different combinations during the SDS-PAGE, which makes it challenging for quantification [59]. Also, the measurement of band intensities is only semi-quantitative. The MPO concentration used in cell viability experiments cannot be compared directly to that in the *ex-vitro* experiments, as the interaction of edaravone with MPO in the cellular system involves cellular uptake and interaction with other proteins.

## 5. Conclusion

Edaravone is a novel antioxidant drug approved for the treatment of

stroke and ALS. Research of its pharmacological effects has mainly been focused on its antioxidant activity. In this report, we have provided evidence that edaravone serves as a peroxidase substrate of MPO, and that this is likely facilitated by acting as an efficient donor substrate for the peroxidase cycle of MPO (Fig. 10). The consequence of donating electrons results in edaravone carbon-centred radicals; though the latter, or its dimerized products, do not appear to adversely affect cells or GSH oxidation significantly (Fig. 11). Most importantly, our study elucidated that edaravone exerts a concentration-dependent biphasic effect on the MPO/ $H_2O_2$ / $Cl^-$  system to modulate the rate of toxic HOCl production and consequent  $H_2O_2$ -induced HL-60 cell death. Further studies should be carried out to expand our knowledge about the intracellular effect of edaravone in HOCl-mediated oxidative stress, and to determine if MPO modulation by edaravone is a functional mechanism of action *in vivo*.

## Acknowledgements

The authors acknowledge funding support from the Natural Sciences and Engineering Research Council (NSERC) grant number RGPIN-2014-04878.

## References

- [1] J.D. Rothstein, Edaravone: a new drug approved for ALS, *Cell* 171 (4) (2017) 725 doi: S0092-8674(17)31198-4 [pii].
- [2] K. Dangerfield, ALS drug approved by health Canada could slow down progression of fatal disease, Available from: <https://globalnews.ca/news/4519791/health-canada-approves-als-drug-radica/>, (Oct 5th, 2019), Accessed date: 1 March 2019.
- [3] C.L. Allen, U. Bayraktutan, Oxidative stress and its role in the pathogenesis of ischaemic stroke, *Int. J. Stroke* 4 (6) (2009) 461–470, <https://doi.org/10.1111/j.1747-4949.2009.00387.x> [doi].
- [4] I. Olmez, H. Ozyurt, Reactive oxygen species and ischemic cerebrovascular disease, *Neurochem. Int.* 60 (2) (2012) 208–212, <https://doi.org/10.1016/j.neuint.2011.11.009> [doi].
- [5] M.M. Gaschler, B.R. Stockwell, Lipid peroxidation in cell death, *Biochem. Biophys. Res. Commun.* 482 (3) (2017) 419–425 doi: S0006-291X(16)31771-5 [pii].
- [6] S.C. Barber, R.J. Mead, P.J. Shaw, Oxidative stress in ALS: a mechanism of neurodegeneration and a therapeutic target, *Biochim. Biophys. Acta* 1762 (11–12) (2006) 1051–1067 doi: S0925-4439(06)00052-4 [pii].
- [7] Y. Yamamoto, T. Kuwahara, K. Watanabe, K. Watanabe, Antioxidant activity of 3-methyl-1-phenyl-2-pyrazolin-5-one, *Redox Rep.* 2 (5) (1996) 333–338, <https://doi.org/10.1080/13510002.1996.11747069> [doi].
- [8] O. Tokumaru, Y. Shuto, K. Ogata, et al., Dose-dependency of multiple free radical-scavenging activity of edaravone, *J. Surg. Res.* 228 (2018) 147–153 doi: S0022-4804(18)30185-9 [pii].
- [9] E. Kamogawa, Y. Sueishi, A multiple free-radical scavenging (MULTIS) study on the antioxidant capacity of a neuroprotective drug, edaravone as compared with uric acid, glutathione, and trolox, *Bioorg. Med. Chem. Lett* 24 (5) (2014) 1376–1379, <https://doi.org/10.1016/j.bmcl.2014.01.045> [doi].
- [10] K. Watanabe, M. Tanaka, S. Yuki, M. Hirai, Y. Yamamoto, How is edaravone effective against acute ischemic stroke and amyotrophic lateral sclerosis? *J. Clin. Biochem. Nutr.* 62 (1) (2018) 20–38, <https://doi.org/10.3164/jcbs.17-62> [doi].
- [11] R. Radi, Peroxynitrite, a stealthy biological oxidant, *J. Biol. Chem.* 288 (37) (2013) 26464–26472, <https://doi.org/10.1074/jbc.R113.472936> [doi].

- [12] A. Fujisawa, Y. Yamamoto, Edaravone, a potent free radical scavenger, reacts with peroxynitrite to produce predominantly 4-NO-edaravone, *Redox Rep.* 21 (3) (2016) 98–103, <https://doi.org/10.1179/1351000215Y.0000000025> [doi].
- [13] S.J. Klebanoff, Myeloperoxidase: friend and foe, *J. Leukoc. Biol.* 77 (5) (2005) 598–625.
- [14] J. Schultz, K. Kaminker, Myeloperoxidase of the leucocyte of normal human blood. I. content and localization, *Arch. Biochem. Biophys.* 96 (3) (1962) 465–467, [https://doi.org/10.1016/0003-9861\(62\)90321-1](https://doi.org/10.1016/0003-9861(62)90321-1) <https://www.sciencedirect.com/science/article/pii/0003986162903211>.
- [15] K.E. Brown, E.M. Brunt, J.W. Heinecke, Immunohistochemical detection of myeloperoxidase and its oxidation products in kupffer cells of human liver, *Am. J. Pathol.* 159 (6) (2001) 2081–2088, [https://doi.org/10.1016/S0002-9440\(10\)63059-3](https://doi.org/10.1016/S0002-9440(10)63059-3) <https://www.sciencedirect.com/science/article/pii/S0002944010630593>.
- [16] P.S. Green, A.J. Mendez, J.S. Jacob, et al., Neuronal expression of myeloperoxidase is increased in alzheimer's disease, *J. Neurochem.* 90 (3) (2004) 724–733, <https://doi.org/10.1111/j.1471-4159.2004.02527.x> [doi].
- [17] R.M. Nagra, B. Becher, W.W. Tourtellotte, et al., Immunohistochemical and genetic evidence of myeloperoxidase involvement in multiple sclerosis, *J. Neuroimmunol.* 78 (1–2) (1997) 97–107, [https://doi.org/10.1016/S0165-5728\(97\)00089-1](https://doi.org/10.1016/S0165-5728(97)00089-1) <https://www.ncbi.nlm.nih.gov/pubmed/9307233>.
- [18] S.J. Klebanoff, Myeloperoxidase: friend and foe, *J. Leukoc. Biol.* 77 (5) (2005) 598–625 doi: jlb.1204697 [pii].
- [19] B.S. van der Veen, M.P. de Winther, P. Heeringa, Myeloperoxidase: molecular mechanisms of action and their relevance to human health and disease, *Antioxidants Redox Signal.* 11 (11) (2009) 2899–2937, <https://doi.org/10.1089/ARS.2009.2538> [doi].
- [20] R.S. Ray, A. Katyal, Myeloperoxidase: bridging the gap in neurodegeneration, *Neurosci. Biobehav. Rev.* 68 (2016) 611–620 doi: S0149-7634(16)30048-3 [pii].
- [21] A. Daugherty, J.L. Dunn, D.L. Rateri, J.W. Heinecke, Myeloperoxidase, a catalyst for lipoprotein oxidation, is expressed in human atherosclerotic lesions, *J. Clin. Invest.* 94 (1) (1994) 437–444, <https://doi.org/10.1172/JCI117342> [doi].
- [22] C.C. Winterbourn, R. Senthilmohan, V.A. Cameron, et al., Plasma concentrations of myeloperoxidase predict mortality after myocardial infarction, *J. Am. Coll. Cardiol.* 49 (20) (2007) 1993–2000, <https://doi.org/10.1016/j.jacc.2007.02.040> <https://www.clinicalkey.es/playcontent/1-s2.0-S0735109707008340>.
- [23] I. Cascorbi, S. Henning, J. Brockmoller, et al., Substantially reduced risk of cancer of the aerodigestive tract in subjects with variant -463A of the myeloperoxidase gene, *Cancer Res.* 60 (3) (2000) 644–649 <http://cancerres.aacrjournals.org/cgi/content/abstract/60/3/644>.
- [24] J. Ahn, M.D. Gammon, R.M. Santella, et al., Myeloperoxidase genotype, fruit and vegetable consumption, and breast cancer risk, *Cancer Res.* 64 (20) (2004) 7634–7639, <https://doi.org/10.1158/0008-5472.CAN-04-1843> <http://cancerres.aacrjournals.org/cgi/content/abstract/64/20/7634>.
- [25] W.F. Reynolds, E. Chang, D. Douer, E.D. Ball, V. Kanda, An allelic association implicates myeloperoxidase in the etiology of acute promyelocytic leukemia, *Blood* 90 (7) (1997) 2730–2737 <https://www.ncbi.nlm.nih.gov/pubmed/9326240>.
- [26] P. Wheatley-Price, K. Asomaning, A. Reid, et al., Myeloperoxidase and superoxide dismutase polymorphisms are associated with an increased risk of developing pancreatic adenocarcinoma, *Cancer* 112 (5) (2008) 1037–1042, <https://doi.org/10.1002/cncr.23267> <https://onlinelibrary.wiley.com/doi/abs/10.1002/cncr.23267>.
- [27] D. Choi, S. Pennathur, C. Perier, et al., Ablation of the inflammatory enzyme myeloperoxidase mitigates features of Parkinson's disease in mice, *J. Neurosci.* 25 (28) (2005) 6594–6600, <https://doi.org/10.1523/JNEUROSCI.0970-05.2005> <http://www.jneurosci.org/cgi/content/abstract/25/28/6594>.
- [28] H.J. Grone, E.F. Grone, E. Malle, Immunohistochemical detection of hypochlorite-modified proteins in glomeruli of human membranous glomerulonephritis, *Lab. Invest.* 82 (1) (2002) 5–14.
- [29] P. Heeringa, R.A. Matthijssen, C.J. Peutz-Kootstra, et al., Myeloperoxidase is critically involved in the induction of organ damage after renal ischemia reperfusion, *Am. J. Pathol.* 171 (6) (2007) 1743–1752, <https://doi.org/10.2353/ajpath.2007.070184> <https://www.clinicalkey.es/playcontent/1-s2.0-S0002944010624376>.
- [30] A.J. Kettle, T. Chan, I. Osberg, et al., Myeloperoxidase and protein oxidation in the airways of young children with cystic fibrosis, *Am. J. Respir. Crit. Care Med.* 170 (12) (2004) 1317–1323, <https://doi.org/10.1164/rccm.200311-1516OC> <http://ajrccm.atsjournals.org/cgi/content/abstract/170/12/1317>.
- [31] P.G. Furtmuller, W. Jantschko, G. Regelsberger, C. Jakopitsch, N. Moguilevsky, C. Obinger, A transient kinetic study on the reactivity of recombinant unprocessed monomeric myeloperoxidase, *FEBS Lett.* 503 (2–3) (2001) 147–150 S0014-5793(01)02725-9 [pii].
- [32] L.K. Folkes, L.P. Candeias, P. Wardman, Kinetics and mechanisms of hypochlorous acid reactions, *Arch. Biochem. Biophys.* 323 (1) (1995) 120–126 doi: S0003-9861(85)70017-3 [pii].
- [33] E.G. Janzen, H.J. Stronks, C.M. Dubose, J.L. Poyer, P.B. McCay, Chemistry and biology of spin-trapping radicals associated with halocarbon metabolism in vitro and in vivo, *Environ. Health Perspect.* 64 (1985) 151–170, <https://doi.org/10.1289/ehp.8564151> [doi].
- [34] R.P. Dash, R.J. Babu, N.R. Srinivas, Two decades-long journey from riluzole to edaravone: revisiting the clinical pharmacokinetics of the only two amyotrophic lateral sclerosis therapeutics, *Clin. Pharmacokinet.* 57 (11) (2018) 1385–1398, <https://doi.org/10.1007/s40262-018-0655-4> [doi].
- [35] Novel ALS therapy edaravone considered for approval in europe, <https://www.thepharmaletter.com/article/novel-als-therapy-edaravone-to-be-considered-for-approval-in-europe>, (2018) , Accessed date: 1 March 2019Updated.
- [36] S. Fujishima, N. Aikawa, Neutrophil-mediated tissue injury and its modulation, *Intensive Care Med.* 21 (3) (1995) 277–285, <https://doi.org/10.1007/BF01701489> <https://www.ncbi.nlm.nih.gov/pubmed/7790621>.
- [37] T. Yang, Y.F. Mao, S.Q. Liu, et al., Protective effects of the free radical scavenger edaravone on acute pancreatitis-associated lung injury, *Eur. J. Pharmacol.* 630 (1–3) (2010) 152–157, <https://doi.org/10.1016/j.ejphar.2009.12.025> [doi].
- [38] K. Ito, H. Ozasa, Y. Noda, S. Arii, S. Horikawa, Effects of free radical scavenger on acute liver injury induced by d-galactosamine and lipopolysaccharide in rats, *Hepatol. Res. : Off. J. Jpn. Soc. Hepatol.* 38 (2) (2008), <https://doi.org/10.1111/j.1872-034X.2007.00252.x> <https://www.ncbi.nlm.nih.gov/pubmed/17727650>.
- [39] J.M. Pullar, M.C. Vissers, C.C. Winterbourn, Living with a killer: the effects of hypochlorous acid on mammalian cells, *IUBMB Life* 50 (4–5) (2000) 259–266, <https://doi.org/10.1080/713803731> [doi].
- [40] M.J. Davies, C.L. Hawkins, D.I. Pattison, M.D. Rees, Mammalian heme peroxidases: from molecular mechanisms to health implications, *Antioxidants Redox Signal.* 10 (7) (2008) 1199–1234, <https://doi.org/10.1089/ars.2007.1927> [doi].
- [41] D.B. Learn, V.A. Fried, E.L. Thomas, Taurine and hypotaurine content of human leukocytes, *J. Leukoc. Biol.* 48 (2) (1990) 174–182.
- [42] E.L. Thomas, M.B. Grisham, M.M. Jefferson, Cytotoxicity of chloramines, *Methods Enzymol.* 132 (1986) 585–593.
- [43] L.P. Candeias, K.B. Patel, M.R. Stratford, P. Wardman, Free hydroxyl radicals are formed on reaction between the neutrophil-derived species superoxide anion and hypochlorous acid, *FEBS Lett.* 333 (1–2) (1993) 151–153 doi: 0014-5793(93)80394-A [pii].
- [44] J.R. Kanofsky, J. Wright, G.E. Miles-Richardson, A.I. Tauber, Biochemical requirements for singlet oxygen production by purified human myeloperoxidase, *J. Clin. Invest.* 74 (4) (1984) 1489–1495, <https://doi.org/10.1172/JCI111562> [doi].
- [45] A.J. Kettle, B.M. Clark, C.C. Winterbourn, Superoxide converts indigo carmine to isatin sulfonic acid: implications for the hypothesis that neutrophils produce ozone, *J. Biol. Chem.* 279 (18) (2004) 18521–18525, <https://doi.org/10.1074/jbc.M400334200> [doi].
- [46] AZD5904 mechanism of action: myeloperoxidase (MPO) inhibitor, <https://openinnovation.astrazeneca.com/azd5904.html> , Accessed date: 1 March 2019.
- [47] A.K. Tiden, T. Sjogren, M. Svensson, et al., 2-thioxanthines are mechanism-based inactivators of myeloperoxidase that block oxidative stress during inflammation, *J. Biol. Chem.* 286 (43) (2011) 37578–37589, <https://doi.org/10.1074/jbc.M111.266981> [doi].
- [48] P.G. Furtmuller, M. Zederbauer, W. Jantschko, et al., Active site structure and catalytic mechanisms of human peroxidases, *Arch. Biochem. Biophys.* 445 (2) (2006) 199–213 doi: S0003-9861(05)00403-0 [pii].
- [49] M. Lin, Y. Katsumura, K. Hata, Y. Muroya, K. Nakagawa, Pulse radiolysis study on free radical scavenger edaravone (3-methyl-1-phenyl-2-pyrazolin-5-one), *J. Photochem. Photobiol., B* 89 (1) (2007) 36–43 doi: S1011-1344(07)00110-8 [pii].
- [50] S. Ono, K. Okazaki, M. Sakurai, Y. Inoue, Density functional study of the radical reactions of 3-methyl-1-phenyl-2-pyrazolin-5-one (MCI-186): Implication for the biological function of MCI-186 as a highly potent antioxidative radical scavenger, *J. Phys. Chem. A* 101 (20) (1997) 3769–3775.
- [51] K. Chegaev, C. Cema, M. Giorgis, et al., Edaravone derivatives containing NO-donor functions, *J. Med. Chem.* 52 (2) (2009) 574–578, <https://doi.org/10.1021/jm8007008> [doi].
- [52] A.B. Gutman, P.G. Dayton, T.F. Yu, et al., A study of the inverse relationship between pKa and rate of renal excretion of phenylbutazone analogs in man and dog, *Am. J. Med.* 29 (1960) 1017–1033 doi: 0002-9343(60)90082-6 [pii].
- [53] A. Perez-Gonzalez, A. Galano, Ionization energies, proton affinities, and pKa values of a large series of edaravone derivatives: implication for their free radical scavenging activity, *J. Phys. Chem. B* 115 (34) (2011) 10375–10384, <https://doi.org/10.1021/jp2047163> [doi].
- [54] Grace Ka Yan Chan, Tracy L. Kleinheinz, David Peterson, John G. Moffat, A simple high-content cell cycle assay reveals frequent discrepancies between cell number and ATP and MTS proliferation assays, *PLoS One* 8 (5) (2013) e63583, <https://doi.org/10.1371/journal.pone.0063583> <https://www.ncbi.nlm.nih.gov/pubmed/23691072>.
- [55] S.R. Khan, A. Baghdasarian, P.H. Nagar, et al., Proteomic profile of aminoglutethimide-induced apoptosis in HL-60 cells: role of myeloperoxidase and arylamine free radicals, *Chem. Biol. Interact.* 239 (2015) 129–138, <https://doi.org/10.1016/j.cbi.2015.06.020> [doi].
- [56] T. Matsura, M. Kai, Y. Fujii, H. Ito, K. Yamada, Hydrogen peroxide-induced apoptosis in HL-60 cells requires caspase-3 activation, *Free Radic. Res.* 30 (1) (1999) 73–83.
- [57] Brett A. Wagner, Garry R. Buettner, Larry W. Oberley, Christine J. Darby, C. Patrick Burns, Myeloperoxidase is involved in H2O2-induced apoptosis of HL-60 human leukemia cells, *J. Biol. Chem.* 275 (29) (2000) 22461–22469, <https://doi.org/10.1074/jbc.M001434200> <http://www.jbc.org/content/275/29/22461.abstract>.
- [58] H.R. Hope, E.E. Remsen, C. Lewis, et al., Large-scale purification of myeloperoxidase from HL60 promyelocytic cells: characterization and comparison to human neutrophil myeloperoxidase, *Protein Expr. Purif.* 18 (3) (2000) 269–276, <https://doi.org/10.1006/prep.1999.1197> <https://www.sciencedirect.com/science/article/pii/S10465928999197X>.
- [59] K.L. Taylor, J. Pohl, J.M. Kinkade J, Unique autolytic cleavage of human myeloperoxidase. implications for the involvement of active site MET409, *J. Biol. Chem.* 267 (35) (1992) 25282 <http://www.jbc.org/content/267/35/25282.abstract>.